Dynamics of chaotic systems with attractive and repulsive couplings

Yuehua Chen,[1] Jinghua Xiao,[1,*] Weiqing Liu,[2] Lixiang Li,[3,4,5] and Yixian Yang[3,4,5]
[1]*School of Science, Beijing University of Posts and Telecommunications, Beijing 100876, China*
[2]*School of Science, Jiangxi University of Science and Technology, Ganzhou 341000, China*
[3]*Information Security Center, State Key Laboratory of Networking and Switching Technology, Beijing University of Posts and Telecommunications, P.O. Box 145, Beijing 100876, China*
[4]*Key Laboratory of Networking and Information Attack and Defence Technology of Ministry of Education, Beijing University of Posts and Telecommunications, Beijing 100876, China*
[5]*National Engineering Laboratory for Disaster Backup and Recovery, Beijing University of Posts and Telecommunications, Beijing 100876, China*
(Received 20 May 2009; revised manuscript received 1 August 2009; published 14 October 2009)

Together with attractive couplings, repulsive couplings play crucial roles in determining important evolutions in natural systems, such as in learning and oscillatory processes of neural networks. The complex interactions between them have great influence on the systems. A detailed understanding of the dynamical properties under this type of couplings is of practical significance. In this paper, we propose a model to investigate the dynamics of attractive and repulsive couplings, which give rise to rich phenomena, especially for amplitude death (AD). The relationship among various dynamics and possible transitions to AD are illustrated. When the system is in the maximally stable AD, we observe the transient behavior of in-phase (high frequency) and out-of-phase (low frequency) motions. The mechanism behind the phenomenon is given.

DOI: 10.1103/PhysRevE.80.046206 PACS number(s): 05.45.Xt, 05.45.Pq

I. INTRODUCTION

Since the latter half of 20th century, coupled nonlinear dynamical systems arise in many branches of physical, biological, chemical, and social sciences and have been extensively studied [1–3]. Recent researches have explored the effect of coupling in nonlinear systems, which can cause rich phenomena such as complete synchronization, partial synchronization, antiphase synchronization (AS), and so on [4–7]. Among the collective behaviors, amplitude death (AD), which refers to a situation where the coupled oscillators drive each other off their cycles and into an equilibrium solution, was first reported in 1984 [8] and has attracted lots of attentions [9–12].

In chemical and biochemical systems attractive (positive) couplings exist extensively in the normal diffusion processes, while repulsive (negative) couplings appear much less extensive. However, repulsive couplings do exist, and together with attractive couplings repulsive couplings play crucial roles in determining important evolutions in natural systems [13–20]. For example, Ref. [13] studies a pair of neurons in presence of coexistence of excitatory (attractive) and inhibitory (repulsive) synaptic couplings. Qu *et al.* [16] investigate the nonlinear dynamics of excitation-contraction (EC) coupling in cardiac myocytes. In Ref. [17], the authors use a chain of coupled chaotic oscillators with negative feedback and delay modeling the experimental laser system, while in [18] the authors analyze the strong energetic interactions of the alkali metal with coadsorbates in chemical surface reaction, i.e., the attractive interaction with coadsorbed oxygen and the effectively repulsive interaction with coadsorbed nitrogen.

In this study, we develop a model of chaotic systems with two couplings to investigate the dynamics of attractive and repulsive couplings, depending on whether the couplings are both negative, both positive and opposite in sign. The system displays not only chaotic complete synchronization (CS) but also periodic antiphase synchronization (PAS), antisynchronous AD, and so on. The relationship of different dynamics and transition process to AD are considered. In addition, a distinctive phenomenon is observed that when the system is in the maximally stable AD, namely, the largest Lyaponov exponent is local minimum, the phase difference between the subsystems oscillating into AD changes from being in-phase to being out-of-phase, and their common frequency undergoes a sharp jump. This phenomenon has also been observed in time-delay-coupled nonlinear systems [11,12]. Further, the reason of phase difference change is analyzed, which is an open problem in their papers.

II. MODEL AND DYNAMICS

In order to investigate the effect of attractive and repulsive couplings, we consider the following model of two identical Lorenz systems [differentiated by subscript 1 or 2, i.e., $\boldsymbol{U_1}=(x_1,y_1,z_1)$ and $\boldsymbol{U_2}=(x_2,y_2,z_2)$]:

$$\dot{x}_1 = \alpha(y_1 - x_1) + \varepsilon_1(x_2 - x_1),$$

$$\dot{y}_1 = \rho x_1 - y_1 - x_1 z_1 + \varepsilon_2(y_2 - y_1),$$

$$\dot{z}_1 = x_1 y_1 - \beta z_1,$$

$$\dot{x}_2 = \alpha(y_2 - x_2) + \varepsilon_1(x_1 - x_2),$$

$$\dot{y}_2 = \rho x_2 - y_2 - x_2 z_2 + \varepsilon_2(y_1 - y_2),$$

*jhxiao@bupt.edu.cn

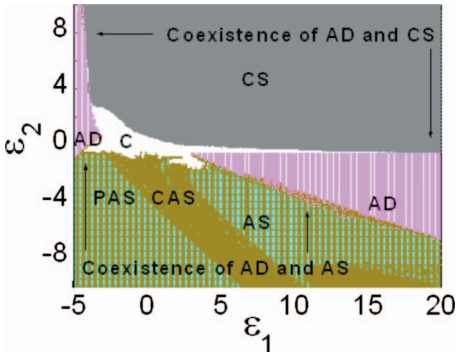

FIG. 1. (Color) Schematic phase diagram for Eq. (1) in the $(\varepsilon_1,\varepsilon_2)$ plane. The white region, the upper gray region, the nether dark yellow region, and the two magenta deltoid regions correspond to C, CS, AS, and AD, respectively, while in AS the portion covered with blue dots corresponds to PAS and the rest corresponds to CAS. The coexistence regions of AD and CS (AS) are indicated by the arrows.

$$\dot{z}_2 = x_2 y_2 - \beta z_2, \tag{1}$$

which are symmetrically coupled through x_1 and x_2, y_1, and y_2. The coupling parameters ε_1 and ε_2 are treated as variables. In the absence of coupling, the subsystems are in the chaotic state when the parameters $\alpha=10$, $\rho=28$, and $\beta=1$ [21].

Make ε_1 as x axis and ε_2 as y axis. For finite coupling strength various dynamics are observed. We can obtain four quadrants based on different values of the coupling parameters ε_1 and ε_2, which can be positive or negative, respectively. The two-dimensional phase space can be observed instead of a line given a coupling parameter which has been deeply investigated theoretically and experimentally. For each pair of coupling parameter $(\varepsilon_1,\varepsilon_2)$, the dynamics of the system is indicated in the schematic Fig. 1 within a representative range of coupling parameters ε_1 and ε_2. The system behaves three primary features: desynchronized chaos (C), CS, and AS, where AS contains PAS, chaotic AS (CAS) and antisynchronous AD. In Fig. 1, the white region corresponds to C. The upper gray region corresponds to CS and here the subsystems are in synchronous chaos. The region, which is shade dark yellow, corresponds to AS embedded with some periodic state windows (PAS) (marked with blue dots). In the two magenta deltoid regions on the left and right respectively the system undergoes AD state. Some special regions, i.e., bistability regions of AD and other dynamics, are marked out, a detailed analysis of which is in Secs. III and IV. Trajectories of oscillator 1 (solid black line) and oscillator 2 (dashed red line) at $(\varepsilon_1,\varepsilon_2)=(0.5,2)$, $(\varepsilon_1,\varepsilon_2)=(0.5,-2)$, $(\varepsilon_1,\varepsilon_2)=(0.5,-5)$ and $(\varepsilon_1,\varepsilon_2)=(-4,2)$ are shown in Figs. 2(a)–2(d), respectively. In Fig. 2(a) the two trajectories overlap since they are in CS. CAS and PAS are shown in Figs. 2(b) and 2(c), respectively. The common frequency of PAS is relatively faster. In Fig. 2(d), amplitude death occurs. The two subsystems settle onto one of two complete reversed values at random, since they are symmetrical coupled identical oscillators.

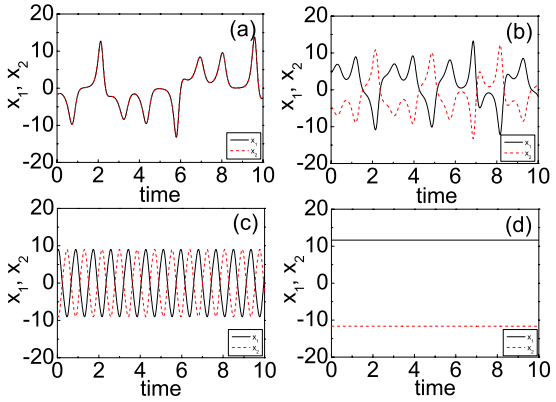

FIG. 2. (Color online) Time series of x_1 (solid black line) and x_2 (dashed red line) (a) of CS with $(\varepsilon_1,\varepsilon_2)=(0.5,2)$, (b) of CAS with $(\varepsilon_1,\varepsilon_2)=(0.5,-2)$, (c) of PAS with $(\varepsilon_1,\varepsilon_2)=(0.5,-5)$, and (d) of AD with $(\varepsilon_1,\varepsilon_2)=(-4,2)$.

In the first (third) quadrant of Fig. 1 both ε_1 and ε_2 are positive (negative) and we observe in-phase (antiphase) synchronization for sufficiently large coupling intensities, and these results are reasonably predictable. Interestingly, the behaviors of the second quadrant (positive ε_2 and negative ε_1) is slightly different from that of the fourth quadrant (positive ε_1 and negative ε_2). Actually, variables x and y are asymmetric in Lorenz system, so the two corresponding couplings (ε_1 and ε_2) are not symmetric, and they have different influences on the synchronization behavior. We can see from Fig. 1 that the coupling of y (ε_2) itself is sufficient to achieve in-phase synchronization (approximately at $\varepsilon_2>1$) and antiphase synchronization (approximately at $\varepsilon_2<-1$) in the absence of the coupling of x ($\varepsilon_1=0$). On the other hand, the influence of x coupling (ε_1) itself is rather weak. Only with large coupling intensity the system can achieve in-phase synchronization (approximately at $\varepsilon_1>4$) and antiphase synchronization (antisynchronous AD here) (approximately at $\varepsilon_1<-4$) in the absence of the coupling of y ($\varepsilon_2=0$). Therefore, in Eq. (1) ε_2 primarily determines in-phase and antiphase synchronization, while ε_1 influences other rich behaviors such as amplitude death, bistabilities, desynchronous chaos, and so on.

III. COEXISTENCE OF CS AND AD PHENOMENON

In Fig. 1, we can see some special regions, where CS and antisynchronous AD coexist. To affirm it, the stability analyses are presented to determine the parameter range for AD and CS states, respectively. First we consider the stable region of fixed points for Eq. (1). Apart from the fixed point at the origin (0, 0, 0, 0, 0, 0), there are several sets of fixed points for the system, but only the reversed pair $(x_1^*,y_1^*,z_1^*, -x_1^*,-y_1^*,z_1^*)$ is possible to be stable, given by

$$x_1^* = \pm\sqrt{\alpha\beta\rho/(\alpha+2\varepsilon_1)-\beta(1+2\varepsilon_2)},$$

$$y_1^* = \pm(1+2\varepsilon_1/\alpha)x_1^*,$$

$$z_1^* = x_1^* y_1^*/\beta,$$

where ε_1 and ε_2 are treated as variables.

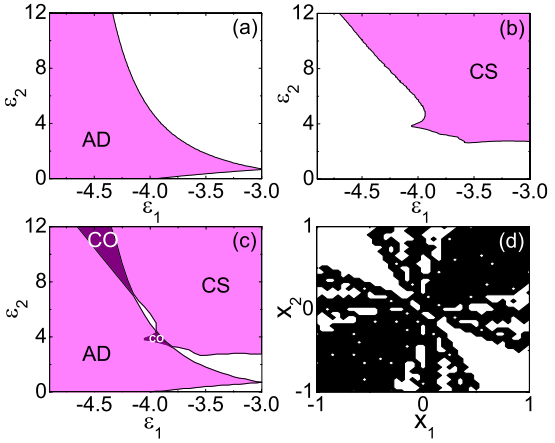

FIG. 3. (Color online) (a) The diagram of the stable region of the antisynchronous fixed point for Eq. (1) (painted magenta) in the $\varepsilon_1-\varepsilon_2$ plane. (b) The diagram of the stable region of CS (painted magenta) in the $\varepsilon_1-\varepsilon_2$ plane. (c) The overlapped diagram of (a) and (b). The two dark magenta regions marked CO are the regions of bistability. (d) The attraction basins for two attractors at $(\varepsilon_1,\varepsilon_2)=(-4.4,10)$. The black areas denote the initial values leading to CS, and the white areas denote the initial values leading to AD. The x axis presents the initial values of x_1 and the y axis presents that of x_2. We fix the initial values of y_1, y_2, z_1, and z_2 are equal to zero.

The eigenvalue matrix H is in the form

$$H=\begin{pmatrix} -\alpha-\varepsilon_1 & \alpha & 0 & \varepsilon_1 & 0 & 0 \\ \rho-z_1^* & -1-\varepsilon_2 & -x_1^* & 0 & \varepsilon_2 & 0 \\ y_1^* & x_1^* & -\beta & 0 & 0 & 0 \\ \varepsilon_1 & 0 & 0 & -\alpha-\varepsilon_1 & \alpha & 0 \\ 0 & \varepsilon_2 & 0 & \rho-z_2^* & -1-\varepsilon_2 & -x_2^* \\ 0 & 0 & 0 & y_2^* & x_2^* & -\beta \end{pmatrix}.$$

Using MATLAB we can easily obtain the eigenvalues of the fixed point during different parameters. If and only if the largest real part of eigenvalues is negative, the fixed point is stable, which corresponds to AD; otherwise the fixed point is unstable. The stable region (painted magenta) of the fixed point is shown in Fig. 3(a) in the $\varepsilon_1-\varepsilon_2$ plane. Here, AD is born via a Hopf bifurcation because a pair of conjugate complex eigenvalues of the fixed point cross the imaginary axis of the complex plane from right to left, or say that the real parts become negative and the pair of imaginary parts are nonzero. And then we compute the conditional Lyapunov exponents for the system on the synchronous manifold $\boldsymbol{M}$, where $\boldsymbol{M}=\{(\boldsymbol{U_1},\boldsymbol{U_2}):\boldsymbol{U_1}=\boldsymbol{U_2}\}$. Similarly, CS is stable if and only if the largest conditional Lyapunov exponent is negative. In Fig. 3(b), we present the stability boundary, which separates the stable region (painted magenta) of CS from the unstable region (painted white). Seen from the overlapped diagram shown in Fig. 3(c), the bistable regions where CS and AD coexist are obtained analytically, which coincide with the numerical result. In the bistable regions, the attraction basins for two attractors are shown in Fig. 3(d).

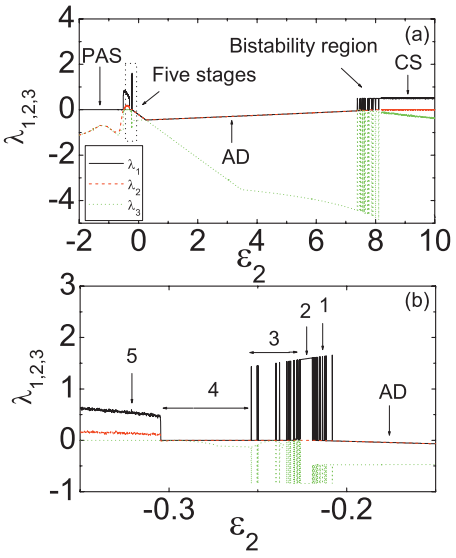

FIG. 4. (Color) (a) The spectrum of the three largest Lyapunov exponents (black solid, red dashed, and green dotted lines corresponding to λ_1, λ_2 and λ_3, respectively) with ε_2 at fixed $\varepsilon_1=-4.2$. From AD($\lambda_1=\lambda_2<0$) to CS($\lambda_1>0,\lambda_2\leq 0$) there is a bistable region (say from $\varepsilon_2=7.36$ to $\varepsilon_2=8.16$). From PAS($\lambda_1=0,\lambda_2<0$) to AD the system undergoes five transition stages (boxed). (b) The enlarged view of the boxed region in (a). 1, the coexisting state of CAS($\lambda_1>0,\lambda_2\leq 0$) and AD. 2, the CAS state. 3, the coexisting state of CAS and QP($\lambda_1=\lambda_2=0$). 4, the QP state. 5, the chaotic state ($\lambda_1>0,\lambda_2>0$).

IV. INSTABILITY PROCESS OF AD

Based on the results above, as a function of ε_2, during the transition from AD to CS the system definitely undergoes either bistable region or chaotic region, in that AD is antisynchronous in this case. The three largest Lyapunov exponents as a function of ε_2 at fixed $\varepsilon_1=-4.2$ are shown in Fig. 4(a), denoted by λ_1, λ_2, and λ_3 respectively. From $\varepsilon_2=-0.22$ to $\varepsilon_2=8.16$, the system is in AD($\lambda_1=\lambda_2<0$), in which we can see a local minimum at $\varepsilon_{2c}=0.25$. Between $\varepsilon_2=7.36$ and $\varepsilon_2=8.16$, the wild fluctuations of the Lyapunov exponent correspond to bistable region where CS($\lambda_1>0,\lambda_2\leq 0$) and AD coexist. The dynamics during the road from AD to PAS($\lambda_1=0,\lambda_2<0$) is relatively rich, which can be seen through the enlarged diagram of Lyapunov exponents [see Fig. 4(b)]. It is interesting to find out that the system undergoes five transition stages as follows: (1) the coexisting state of CAS($\lambda_1>0,\lambda_2\leq 0$) and AD, (2) the CAS state, (3) the coexisting state of CAS and quasiperiodicity ($\lambda_1=\lambda_2=0$) (QP), (4) the QP state, and (5) the chaotic state ($\lambda_1>0,\lambda_2>0$), where these stages do not always appear together at other values of ε_1.

Though the shapes of AD domains in the second quadrant and the fourth quadrant are rather different, the AD behaviors found in both quadrants are basically the same. From Fig. 1, it is evident that there is bistability region of AD and AS in the fourth quadrant; moreover, there is also bistability region between AD and CS in the fourth quadrant.

V. ANALYSIS ON THE PHASE DIFFERENCE CHANGE

Before and after the minimum of λ_1 ($\varepsilon_{2c}=0.25$), the transient trajectories of the two subsystems going into complete

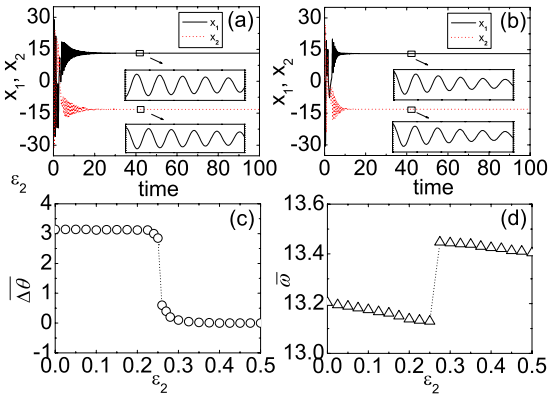

FIG. 5. (Color online) Time series of x_1 (solid black) and x_2 (dotted red) going into AD, (a) at $\varepsilon_2=0$ (out of phase) and (b) at $\varepsilon_2=0.5$ (in phase), at fixed $\varepsilon_1=-4.2$. The values are accurate to the eighth place after decimal point. The four smaller graphs in (a) and (b) enlarge the time series from $t=40$ to $t=42.5$. (c) The average phase difference ($\overline{\Delta\theta}$) between subsystems as a function of ε_2. (d) Numerically calculated average common frequency ($\bar{\omega}$) with ε_2.

AD are shown in Fig. 5(a) for $\varepsilon_2=0$ and (b) for $\varepsilon_2=0.5$ at fixed $\varepsilon_1=-4.2$, respectively. A dramatic change can be seen in two aspects (compare the smaller graphs inside): phase difference between the two subsystems ($\overline{\Delta\theta}$) which is defined as $\overline{\Delta\theta}=\langle|\theta_1-\theta_2|\rangle$ where $\langle\cdot\rangle$ denotes the average over time while $\theta_i=\tan^{-1}[(y_i-y_i^*)/(x_i-x_i^*)]$ and common frequency ($\bar{\omega}$) which is measured from peak-to-peak separation and averaged over time [11,22]. At $\varepsilon_2=0$ the phase difference is π (out of phase), while at $\varepsilon_2=0.5$ the phase difference is zero (in-phase). The phase difference ($\overline{\Delta\theta}$) is shown as a function of ε_2 in Fig. 5(c). This clearly suggests the transition of the phase difference from π to zero across the change parameter ($\varepsilon_{2c}=0.25$). The common frequency ($\bar{\omega}$) is shown as a function of ε_2 in Fig. 5(d). The step-like change corresponds to the jump of common frequency of the system.

Similar phenomenon in phase difference and common frequency was first observed in time-delay-coupled chaotic oscillators in Ref. [11]. The author gave out the reason of frequency jump via time-delay-coupled limit cycles system, that is due to a jump in the imaginary part of the eigenvalue of the fixed point. Following [11], the transient behaviors were further explored in Ref. [12]. The authors explained that the phase difference can be either zero or π across the change parameter. However the reason leading to phase difference change remains to be settled.

In order to understand the underlying mechanism, we first review all the eigenvalues of the fixed point for Eq. (1) nearby $\varepsilon_{2c}=0.25$. It is well known that the behaviors of the fixed point are influenced by all the eigenvalues jointly, in which the relatively large eigenvalues play the dominant roles. Here, the magnitude of eigenvalues is determined by comparing the magnitude of their real parts. The front four largest eigenvalues appear in way of two pairs of conjugate complex eigenvalues. The real parts of eigenvalues are shown in Fig. 6(a) along with ε_2 at fixed $\varepsilon_1=-4.2$. The red and blue lines correspond to real parts of a pair of conjugate complex eigenvalues, denoted by Re_{o1} and Re_{o2}, respectively, where $Re_{o1}=Re_{o2}$ for conjugate. The green and black

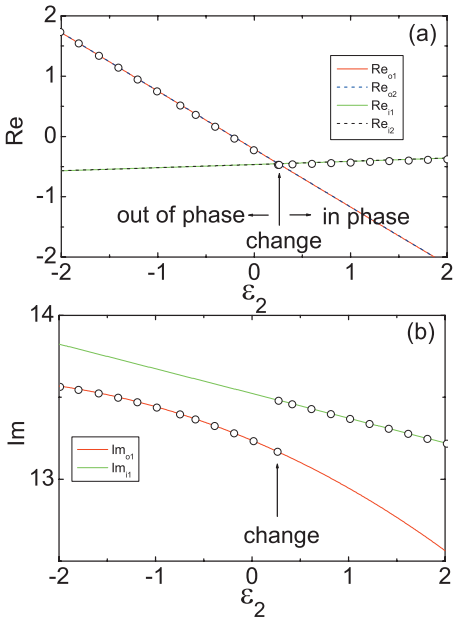

FIG. 6. (Color) (a) The real parts of the four largest eigenvalues along with ε_2 at fixed $\varepsilon_1=-4.2$. Red and blue lines correspond to the real parts of a pair of conjugate complex eigenvalues, respectively, denoted by Re_{o1} and Re_{o2}. Green and black lines correspond to the real parts of another pair, respectively, denoted by Re_{i1} and Re_{i2}. The largest real part Re_1 is shown by circles. The cross point of the two pairs of real parts are indicated by the vertical arrow, at $\varepsilon_{2c}=0.25$, where Re_1 has a local minimum. (b) The imaginary parts corresponding to the real parts in (a) (the other two imaginary parts omitted owing to symmetry). Red and green lines correspond to Im_{o1} and Im_{i1}, respectively. The vertical arrow shows the parameter value, $\varepsilon_{2c}=0.25$, where Im_1 undergoes a sharp jump.

lines correspond to real parts of another pair, denoted by Re_{i1} and Re_{i2}, respectively, where $Re_{i1}=Re_{i2}$. In Fig. 6(b), the imaginary parts corresponding to Re_{o1} and Re_{i1} are shown, denoted by Im_{o1} (red line) and Im_{i1} (green line), respectively. Because of the symmetry of conjugate complex eigenvalues in their imaginary parts, we just need to display two positive imaginary parts. In addition, the largest real part (Re_1) and the corresponding imaginary part (Im_1) of the eigenvalues are shown by circles in Figs. 6(a) and 6(b), respectively. It is surprising to find that the two pairs of real parts cross each other at $\varepsilon_{2c}=0.25$ [see Fig. 6(a)]. Via the cross, the former smaller pair of real parts exceed the former largest pair and become the largest real parts that means the eigenvalues of the most significant influence on the behavior of fixed point before the cross are replaced by another pair of eigenvalues and the characteristics of the fixed point will change. The switch of the largest real part leads to the corresponding switch of the largest imaginary part. This cross not only explain why the slope of λ_1 has a local minimum but also explain why the imaginary part of the eigenvalue (Im_1) undergoes a sharp jump, which is just the cause of frequency jump. For purpose of proving the function of the cross that leads to the phase difference change, we make a further investigation on the eigenvectors. The eigenvectors corresponding to the eigenvalue $Re_{o1}+i\,Im_{o1}$ and $Re_{i1}+i\,Im_{i1}$ separately can be written as

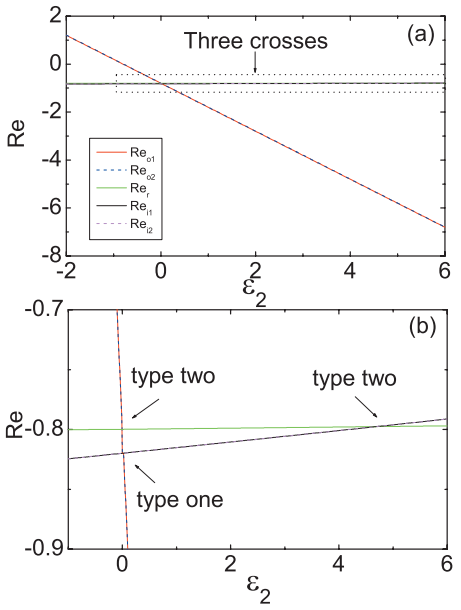

FIG. 7. (Color) (a) The real parts of the five largest eigenvalues which contain a real eigenvalue and two pairs of conjugate complex eigenvalues along with ε_2 at fixed $\varepsilon_1=-4.8$ (red, blue, green, black, and magenta lines corresponding to Re_{o1}, Re_{o2}, Re_r, Re_{i1}, and Re_{i2}, respectively). The boxed region of the curves is enlarged and shown in (b). There are two types of crosses as labeled, which are type one: between real root and complex roots and type two: between two pairs of complex roots. Only the cross of type two can lead to phase difference change.

$$\boldsymbol{V_{o1}} = (c_{o1}, d_{o1}, r_{o1}, -c_{o1}, -d_{o1}, r_{o1})^T,$$

$$\boldsymbol{V_{i1}} = (c_{i1}, d_{i1}, r_{i1}, c_{i1}, d_{i1}, -r_{i1})^T,$$

where c_{o1}, d_{o1}, c_{i1} and d_{i1} are complex numbers and r_{o1} and r_{i1} are real numbers. As expected, in $\boldsymbol{V_{o1}}$, the sign of complex element pairs are opposite, while in $\boldsymbol{V_{i1}}$, the sign of complex element pairs are same. So it is the possible reason for the phase difference transition that a cross in the real parts of two pairs of conjugate complex eigenvalues for the fixed point. Furthermore, in our system the feature of being out-of-phase below $\varepsilon_{2c}=0.25$ and being in-phase above $\varepsilon_{2c}=0.25$ can be visually displayed from the phase diagram (see Fig. 1), i.e., below ε_{2c} the system is apt to AS, above ε_{2c} is CS.

Now it is significant to make a discussion on the case of real eigenvalue occurring cross. At an altered fixed parameter $\varepsilon_1=-4.8$, we consider the front five largest eigenvalues composed of a real eigenvalue and two pairs of conjugate complex eigenvalues. Their real parts are shown in Fig. 7(a) as a function of ε_2. The boxed region of the curves is amplified [see Fig. 7(b)]. We see three crosses, which can be divided into two types: type one (the real parts of a pair of complex eigenvalues cross with that of another pair of complex eigenvalues) and type two (the real parts of a pair of complex eigenvalues cross with that of real eigenvalue). The cross occurring at $\varepsilon_2 \approx 0.02$ belongs to type one, and the crosses occurring at $\varepsilon_2 \approx 0$ and $\varepsilon_2 \approx 4.68$, respectively, belong to type two. Calculating the phase difference around $\varepsilon_2 \approx 4.68$ (type two), there is no transition of in and out of phase motions. It means that a real eigenvalue crossing with a pair of complex eigenvalues will not result in phase difference change.

VI. CONCLUSION

In summary, we have studied the impacts of the interaction between attractive and repulsive couplings on dynamics, which is a meaningful research topic. In cardiac myocyte, the interactions of EC coupling give rise to rich dynamics, in which rapid heart rates may cause lethal arrhythmias. "Recent evidence indicates that dynamics properties of cardiac EC coupling contribute importantly to functional magnification of tissue heterogeneities promoting arrhythmogenesis" [16]. In this paper, we refer ε_1 and ε_2 as attractive and repulsive couplings, respectively. Under this interactions, the coupled chaotic systems mainly displays CS and AS, while the latter appears as CAS, PAS, and AD. At the point of maximum stability in AD we observe the phenomena of phase difference change and frequency jump, previously proposed in coupled chaotic oscillators with time delay [11,12]. We focus on the unsolved issue of the cause for the phase difference change and get a reasonable conclusion that is due to a cross in the real parts of two pairs of conjugate complex eigenvalues. It has certain practical significance to know when the motion goes from being in-phase to being out-of-phase and the common frequency gets fast sharply [23].

The presence and importance of attractive and repulsive couplings are well acknowledged not only in biological systems, such as neurons [13–15], cardiac myocyte [16], but also in other experimental applications, such as laser system [17], chemical reaction [18] and so on. Our study provides potentially useful mechanistic insights to the attractive and repulsive coupling dynamics. We will continue studying the effect of positive and negative feedbacks on large complex networks.

ACKNOWLEDGMENTS

This work is supported by the National Natural Science Foundation of China (Grants No. 60821001 and No. 10575016), the Specialized Research Fund for the Doctoral Program of Higher Education of China (Grant No. 200800131028), the National Basic Research Program of China (973 Program) (Grant No. 2007CB310704), Foundation for the Author of National Excellent Doctoral Dissertation of PR China (FANEDD) (Grant No. 200951), and the 111 Project (Grant No. B08004).

[1] M. Dolnik and I. R. Epstein, Phys. Rev. E **54**, 3361 (1996).
[2] J. D. Murray, *Mathematical Biology*, 2nd ed. (Springer, Berlin, 1993).
[3] A. Hohl, A. Gavrielides, T. Erneux, and V. Kovanis, Phys. Rev. Lett. **78**, 4745 (1997).
[4] L. M. Pecora and T. L. Carroll, Phys. Rev. Lett. **64**, 821 (1990).
[5] G. Hu, Y. Zhang, H. A. Cerdeira, and S. G. Chen, Phys. Rev. Lett. **85**, 3377 (2000).
[6] W. Liu, J. Xiao, X. Qian, and J. Yang, Phys. Rev. E **73**, 057203 (2006).
[7] L. Li, H. Peng, X. Wang, and Y. Yang, Phys. Lett. A **333**, 269 (2004).
[8] Y. Yamaguchi and H. Shimizu, Physica D **11**, 212 (1984).
[9] J. Yang, Phys. Rev. E **76**, 016204 (2007).
[10] W. Liu, J. Xiao, and J. Yang, Phys. Rev. E **72**, 057201 (2005).
[11] A. Prasad, Phys. Rev. E **72**, 056204 (2005).
[12] A. Prasad, J. Kurths, S. K. Dana, and R. Ramaswamy, Phy. Rev. E **74**, 035204(R) (2006).
[13] T. Yanagita, T. Ichinomiya, and Y. Oyama, Phys. Rev. E **72**, 056218 (2005).
[14] M. I. Rabinovich, P. Varona, A. I. Selverston, and H. D. I. Abarbanel, Rev. Mod. Phys. **78**, 1213 (2006).
[15] P.-J. Kim, T.-W. Ko, H. Jeong, and H.-T. Moon, Phys. Rev. E **70**, 065201(R) (2004).
[16] Z. Qu, Y. Shiferaw, and J. N. Weiss, Phys. Rev. E **75**, 011927 (2007).
[17] I. Leyva, E. Allaria, S. Boccaletti, and F. T. Arecchi, Chaos **14**, 118 (2004).
[18] L. Hong, H. Uecker, M. Hinz, L. Qiao, I. G. Kevrekidis, S. Gunther, T. O. Mentes, A. Locatelli, and R. Imbihl, Phys. Rev. E **78**, 055203(R) (2008).
[19] L. S. Tsimring, N. F. Rulkov, M. L. Larsen, and M. Gabbay, Phys. Rev. Lett. **95**, 014101 (2005).
[20] Prashant M. Gade, D. V. Senthilkumar, Sukratu Barve, and Sudeshna Sinha, Phys. Rev. E **75**, 066208 (2007).
[21] Y. Wu, W. Liu, J. Xiao, and M. Zhan, Phys. Lett. A **369**, 464 (2007).
[22] M. G. Rosenblum, A. S. Pikovsky, and J. Kurths, Phys. Rev. Lett. **78**, 4193 (1997).
[23] A. Prasad, Y. Lai, A. Gavrielides, and V. Kovanis, Phys. Lett. A **318**, 71 (2003).